IV. Discussion and Conclusion

The application of the PCA approach to a set of TEAOE recorded at different stimulus levels reduces on average the acquisition time of TEAOE to about one fourth of the time with the classical procedure. The comparison between the *Similitude* values provided statistical evidence that the PCA approach produces no loss of information in the set of data in term of similarity between the rapidly acquired PCA-processed set and the GS set. The use of the PCA approach statistically improves the *Reproducibility* of the set of data both for 60- and 100-sweep averaged data and, hence, the PCA approach improves dramatically the identification of the response in these conditions.

The effectiveness of the procedure resulted very strongly influenced by the number of sweeps of the rapidly acquired set. Hence, it is advisable to apply the approach only to a set of TEAOE averaged over no less than 60 sweeps. On the other hand, the increase of the number of sweeps from 60 to 100 does not produce a statistical significant increase in *Similitude.*

As to the minimum number of TEOAE responses in the set, the PCA approach can be applied to a set of only three recordings at the highest stimuli (83-, 80-, and 77-dB SPL, i.e., the stimulus levels typically used in clinical practice). The PCA processing of this set of only three recordings obtains practically the same results in terms of *Similitude* that can be obtained by PCA processing a set of 11 responses, when the data at the same stimulus levels are compared.

References

[1] D. T. Kemp, "Stimulated acoustic emissions from within the human auditory system," *J. Acoust. Soc. Amer.*, vol. 64, pp. 1386–1391, 1978.

[2] R. Probst, B. L. Lonsbury-Martin, and G. K. Martin, "A review of otoacoustic emissions," *J. Acoust. Soc. Amer.*, vol. 89, pp. 2027–2067, 1991.

[3] F. Grandori and M. E. Lutman, "European consensus statement on neonatal hearing screening. Finalised at the European Consensus Development Conference on Neonatal Hearing Screening, 15–16 May 1998, Milan," *Int. J. Pediatr. Otorhinolaryngol.*, vol. 44, no. 3, pp. 309–310, Aug. 10, 1998.

[4] M. E. Lutman, "Reliable identification of click-evoked otoacoustic emissions using signal-processing techniques," *Br. J. Audiol.*, vol. 27, pp. 103–108, 1993.

[5] P. Ravazzani, G. Tognola, F. Grandori, and J. Ruohonen, "A two-dimensional filter to facilitate detection of transient-evoked otoacoustic emissions," *IEEE Trans. Biomed. Eng.*, vol. 45, pp. 1089–1096, Sept. 1998.

[6] E. M. Glaser and D. S. Ruchkin, *Principal of Neurobiological Signal Analysis*. New York: Academy Press, 1976.

[7] J. Mocks, "Topographiscs components model for event-related potentials and some biophysical considerations," *IEEE Trans. Biomed. Eng.*, vol. 35, pp. 482–484, <**Month?**> 1988.

[8] M. Turk and A. Pentland, "Eigenfaces for recognition," *Journal of Cognitive Neuroscience*, vol. 3, pp. 71–86, 1991.

[9] S. Yamamoto, Y. Suto, H. Kawamura, T. Hashizume, and T. Kakurai, "Quantitative gate evaluation of hip diseases using principal component analysis," *J. Biomech.*, vol. 16, no. 9, pp. 717–726, 1983.

[10] P. Ravazzani and F. Grandori, "Evoked otoacoustic emissions: Nonlinearities and response interpretation," *IEEE Trans. Biomed. Eng.*, vol. 40, pp. 500–504, May 1993.

Doppler Ultrasound Imaging of Magnetically Vibrated Brachytherapy Seeds

Stephen A. McAleavey*, Deborah J. Rubens, and Kevin J. Parker

***Abstract*—Vibration induced by an alternating magnetic field is proposed as a method for the identification of modified brachytherapy seeds with Doppler ultrasound. *In vitro* experiments with agar and liver-tissue phantoms using a clinical scanner and simple apparatus demonstrate that the technique is feasible.**

***Index Terms*—Brchytherapy, Doppler, guidance, prostate, ultrasound.**

I. Introduction

Brachytherapy, the application or implantation of radioactive sources to apply a lethal dose of radiation to surrounding tissues, is widely used to treat prostate and other cancers [1], [2]. A typical source for prostate cancer treatment (called a "seed") is a titanium capsule 0.8 mm in diameter and 4.5 mm in length containing a radioactive element and a radio-opaque marker for identification in computed tomography (CT) and X-ray images. The small tissue volume irradiated requires that seeds be placed accurately to ensure an adequate radiation dose. To that end, transrectal ultrasound is employed to guide the needles used to deposit the seeds in the prostate [3], [4]. Ultrasound is used because of its ability to produce clear images of the prostate capsule, and to follow the insertion of needles in real time [1], [3].

The seeds themselves are often difficult to see in the ultrasound image [5], [6]; their orientation and shape can cause them to produce a weaker echo than might be expected. Furthermore, the presence of other highly echogenic targets (e.g., calcifications, air introduced by the brachytherapy needle, and blood–tissue interfaces created by bleeding) suggests that simply making the target brighter is not necessarily a solution. Due to the difficulties in visualizing seeds with ultrasound, CT is used at present for postoperative assessment of seed placement [5]. It would be advantageous if this assessment could be performed with ultrasound.

Here, a technique is demonstrated by which modified brachytherapy seeds may be identified and differentiated from other echo targets. Brachytherapy seeds that are magnetized or ferromagnetic may be vibrated within an elastic medium by the application of an oscillating external magnetic field. Doppler ultrasound may be used to detect the vibration of the brachytherapy seeds. Vibration amplitudes of a small fraction of the ultrasound wavelength are readily detectable. The unique Doppler signature associated with the modified brachytherapy seeds in the oscillating field allow them to be readily distinguished from other bright scatterers in the prostate. An unmodified clinical scanner with Power Doppler facilities can highlight the vibrating seeds

Manuscript received April 5, 2002; revised April 5, 2002; revised September 29, 2002. This work was supported in part by the University of Rochester Department of Electrical and Computer Engineering and in part by the Rochester Center for Biomedical Ultrasound. *Asterisk indicates corresponding author.*

*S. A. McAleavey was with the Department of Electrical and Computer Engineering, University of Rochester, Rochester, NY 14642 USA. He is now with the Department of Biomedical Engineering, Duke University, Room 136, School of Engineering, Box 90281, Durham, NC 27708 USA (e-mail: stephen.mcaleavey@duke.edu).

D. J. Rubens is with the Department of Radiology, University of Rochester Medical Center, Rochester, NY 14642 USA.

K. J. Parker is with the Department of Electrical Engineering, University of Rochester, Rochester, NY 14627 USA.

Digital Object Identifier 10.1109/TBME.2002.807644

in an ultrasound image and clearly distinguish them from surrounding bright echoes.

II. Theory

A. Particle Motion in a Magnetic Field

An elongated, magnetizable particle (one that is acted upon by a magnetic field, but carries no significant permanent magnetic field of its own) in a magnetic field experiences a torque that tends to align it with the field [7]. This is observed, for instance, when iron filings are scattered on a paper placed atop a magnet; the filings align themselves with the field. The alignment occurs even though the particles themselves are not magnetized, so long as the particle has a discernable anisotropy.

A periodic force applied to particles embedded in an elastic medium will cause them to vibrate about their rest positions. This periodic force may be applied to the particles by an oscillating magnetic field, generated, for instance, by an alternating current in a coil of wire. The field strength is proportional to the current flowing in the coil, and the torque on the particle is proportional to the square of the applied field [7], [8]. Because of the square law dependence of torque on current, the vibration of the particle is twice the frequency of the coil current. The particle receives a torque in the same direction for each half cycle of the current.

A permanently magnetized particle will experience a torque whose direction will depend upon the direction pf the field; reversing the field will reverse the torque. The torque will be proportional to the applied field, and the vibration frequency is equal to the current frequency [7].

B. Doppler Detection

Doppler ultrasound is routinely used to detect and quantify the motion of blood and other tissues [9]. Vibrating objects are not ordinarily the targets of Doppler scans, but small vibrations are easily detectible with Doppler equipment [10], [11]. Vibrations with a frequency of more than a few Hertz produce Doppler signals with unique characteristics, most clearly seen in the pulsed wave (PW) Doppler spectrograph display [9], where vibrating targets result in bands in the spectrograph display at integer multiples of the vibration frequency [11]. Increased vibration amplitude shifts the bands to higher multiples of the vibration frequency. Vibration-induced Doppler signals are readily distinguished from flow-induced signals; their spectral content is symmetric about zero frequency, and the energy is confined to multiples of the vibration frequency.

C. Target Identification

Brachytherapy seeds may be made to vibrate within the prostate under the influence of an external magnetic field by replacing the radio-opaque marker in the seed with iron, a rare-earth magnet, or other suitable magnetic component. Because the proposed modification replaces one radio-opaque material with another, we do not expect our modification to significantly change the appearance of seeds under X-ray or CT. No external modification to the seed is required, though it is certainly possible to place the ferromagnetic component on the outside of the seed. The vibration may be identified with the Power Doppler mode of an ultrasound scanner, which will highlight in color all vibrating targets within the image. Bright scatterers without any ferromagnetic component, such as air bubbles and tissue interfaces, will not vibrate under the influence of the field and will not be illuminated by the Power Doppler display. Judicious selection of coil current and wall-filter cutoff frequencies allows for the rejection of low velocity flow and other Doppler sources. Alternatively, the PW Doppler range gate may be placed over a suspect echo to determine its nature. With the oscillating magnetic field in place, bands will appear in the Doppler spectral display over a seed echo, while no bands will be seen over other echo sources.

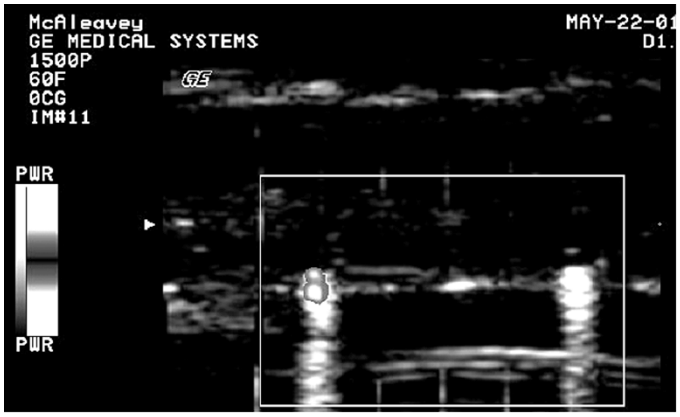

Fig. 1. Power Doppler image of steel (left) and copper (right) seeds in agar. Note the highlighting of the steel seed by Power Doppler, and the absence of a Doppler signal about the copper seed.

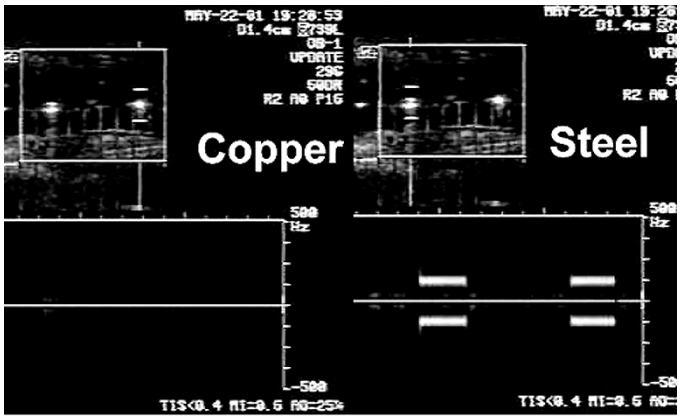

Fig. 2. PW Doppler spectra for the seeds of Fig. 1. A Doppler signal is visible for the steel but not the copper seed.

III. Experiment

An *in vitro* proof-of-concept study has been performed. A coil, consisting of 150 turns of 22-gauge magnet wire on a 10-cm-diameter Lexan shell, coupled to a variable transformer, was used to generate a 60-Hz alternating magnetic field. Phantoms placed within the coil were imaged with a GE Logiq 700MR ultrasound system. A 7-MHz linear array transducer was used. The seeds were oriented with their long axes perpendicular to the scan plane.

Two phantoms were used in the experiments. The first phantom, cast from 3% by weight agar solution, contained copper (0.7-mm diameter) and steel (0.5-mm diameter) wire cut into 4.5-mm-long sections to simulate brachytherapy seeds. The two populations of "seeds" were used to demonstrate the ability to distinguish otherwise identical ferrous and nonferrous targets. The second phantom was a sample of fresh bovine liver tissue from a local butcher, with embedded steel wire seeds. The liver was kept refrigerated but otherwise unpreserved.

Fig. 1 is a typical Power Doppler scan of the agar phantom. The echo on the left is that of a steel wire, that on the right of a copper wire. In the presence of an alternating field, Power Doppler highlights the steel wire alone. Fig. 2 presents PW Doppler spectra for the same targets as Fig. 1. A current of $\sim$10 A at 60 Hz was pulsed through the coil approximately once every other second. With the range gate centered over the steel seed, the appearance of $\pm$120-Hz bands in the spectral

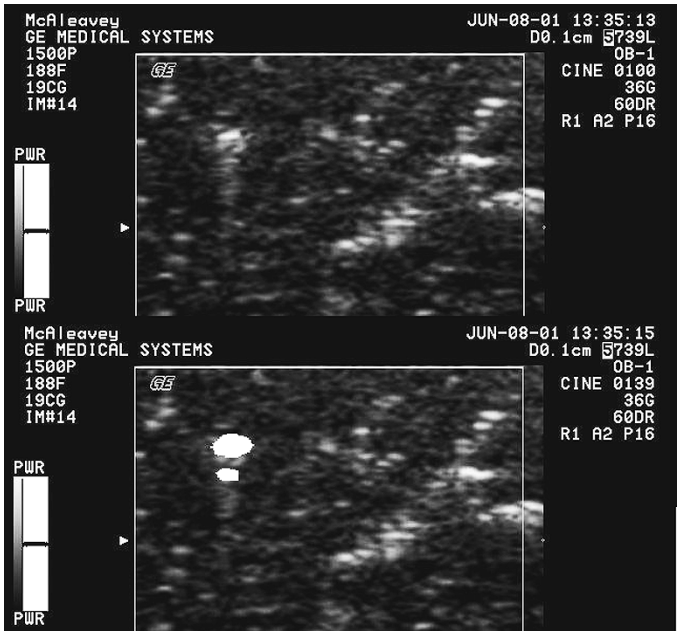

Fig. 3. Power Doppler images of a steel seed in liver with no field (top) and a 60-Hz magnetic field (bottom) applied.

display is noted when the current is switched on. With the range gate over the copper wire, no such bands are seen.

The detection by Doppler of vibration of the steel seed with alternating current applied to the coil and the absence of detectable vibration in the copper seed elucidates two important points. First, the vibration detected is not a microphonic effect. That is, vibrations from the coil are not coupling into the phantom to a significant degree. Were this the case, one would expect to see vibration in both the copper and the steel seeds with the coil activated. Second, these images demonstrate that otherwise similar scatterers are distinguishable based on their magnetic properties.

Images of the liver tissue sample with a seed in frame under Power Doppler are shown in Fig. 3. With the coil off, it is difficult to distinguish the seed from the other echogenic targets in the liver, trapped air and connective tissue. With the coil switched on, a strong Doppler signal is detected and displayed about the seed. A secondary Doppler echo appears behind the seed due to reverberation effects.

IV. Discussion

The potential for powerful magnetic fields to displace the proposed seeds makes compatibility with magnetic resonance (MR) imaging a concern with this technique. Several authors have investigated the potential hazards and artifacts associated with MR imaging of embedded ferromagnetic materials [12]–[14]. It appears that some discretion is involved in terms of the location magnetic material and the strength of displacement forces acting upon it. Shellock concludes [12] that "MR imaging may be performed safely in patients with metallic implants, materials, or devices if the object is nonferromagnetic or is only minimally attracted by the static magnetic field in relation to its *in vivo* application (i.e., the associated deflection force or attraction is insufficient to move or dislodge the implant or material *in situ*)." Thus, as a practical matter certain configurations, such as "open magnet" imaging of the shoulder or brain, may be possible in patients with implanted ferromagnetic brachytherapy seeds.

Another issue in applying this technology is that the orientation of an implanted seed cannot be assumed to be consistent from seed to seed, due to swelling of the prostate and possible migration of the seeds after implantation. Because the seed acts as a strongly specular reflector, an unfavorable orientation can direct most of the seed echo away from the transducer. This is a cause of difficulty in conventional ultrasound imaging of seeds. Fortunately, the vibrating seed induces motion in a small volume of surrounding tissue. Doppler signal processing is exquisitely sensitive to the detection of weak moving scatterers in the presence of stationary clutter. Therefore, while there is an angular sensitivity associated with this technique, seeds can still be detected even in the absence of a strong specular reflection over a wide range of angles.

Most Doppler ultrasound systems are only sensitive to the component of motion which projects onto the beam axis. This gives rise to the concern that the seed will not be detected because the direction of vibration may be lateral to the beam. The orientation of the magnetic field is not fixed, but determined by the coil design. Therefore, reorientation of the coil, or phasing of multiple coils, may be used to sweep the magnetic field orientation and select an optimum. In addition, a gradient field may be applied to create a linear force, rather than a torque. By ensuring that the gradient is in the direction of beam propagation, a detectable Doppler signal may be produced. Finally, ultrasound techniques for lateral motion detection do exist [15], [16]; these may also prove useful in seed detection.

Prostate brachytherapy may involve the implantation of 100 or more seeds. The performance of this method in imaging multiple seeds simultaneously is not considered here. Possible complications include interference from ring-down artifacts and blurring of adjacent seed images. The investigation of these issues will be the subject of future work.

Acknowledgment

The authors are grateful for the comments of the anonymous reviewers.

References

[1] M. D. Rifken, *Ultrasound of the Prostate: Imaging in the Diagnosis and Therapy of Prostatic Disease*, 2nd ed. Philadelphia: Lipponcott-Raven, 1997.

[2] L. W. K. Chung, W. B. Isaacs, and J. W. Simons, *Prostate Cancer: Biology, Genetics, and the New Theraputics*. Totowa, NJ: Humana, 2001.

[3] S. St. C. Carter, S. T. Torp-Pedersen, and H. H. Holm, "Ultrasound Guided Implantation Techniques in Treatment of Prostate Cancer," *Urologic Clin. No. Amer.*, vol. 16, pp. 751–762, Nov. 1989.

[4] H. H. Holm, N. Juul, J. F. Pedersen, H. Hansen, and I. Stroyer, "Transperineal (125) iodine seed implantation in prostatic cancer guided by transrectal ultrasonography," *J. Urol.*, vol. 130, pp. 283–286, Aug. 1983.

[5] C. C. Blake, T. L. Elliot, P. J. Slomka, D. B. Downey, and A. Fenster, "Variability and accuracy of measurements of prostate brachytherapy seed position *in vitro* using three-dimensional ultrasound: An intra- and inter-observer study," *Med. Phys.*, vol. 27, pp. 2788–2795, Dec. 2000.

[6] S. Nag, V. Pak, J. Blasko, and P. D. Grimm, "Brachytherapy for prostate cancer," in *Principles and Practice of Brachytherapy*, S. Nag, Ed. Armonk, NY: Futura, 1997.

[7] T. B. Jones, *Electromechanics of Particles*. New York: Cambridge Univ. Press, 1995.

[8] H. C. O'Hanian, *Modern Physics*. Englewood Cliffs, NJ: Prentice-Hall, 1987.

[9] J. A. Jensen, *Estimation of Blood Velocities Using Ultrasound: A Signal Processing Approach*. Cambridge, UK: Cambridge Univ. Press, 1996.

[10] S. McAleavey, Z. Hah, and K. Parker, "A thin film phantom for blood flow simulation and doppler test," *IEEE Trans. Ultrason., Ferroelect., Freq. Contr.*, vol. 48, pp. 737–742, May 2001.

[11] J. Holen, R. C. Waag, and R. Gramiak, "Representations of rapidly oscillating structures on the Doppler display," *Ultrasound Med. Biol.*, vol. 11, pp. 267–272, Mar./Apr. 1985.

[12] F. G. Shellock and J. S. Curtis, "MR imaging and biomedical implants, materials, and devices: An updated review," *Radiology*, vol. 180, pp. 541–550, 1991.

[13] P. F. J. New, B. R. Rosen, T. J. Brady, F. S. Bounanno, J. P. Kistler, C. T. Burt, W. S. Hinshaw, J. H. Newhouse, G. M. Pohost, and J. M. Taveras, "Potential hazards and artifacts of ferromagnetic and nonferromagnetic surgical and dental materials and devices in nuclear magnetic resonance imaging," *Radiology*, vol. 147, pp. 139–148, April 1983.
[14] G. P. Teitelbaum, W. G. Bradley, Jr., and B. D. Klein, "MR imaging artifacts, ferromagnetism, and magnetic torque of intravascular filters, stents, and coils," *Radiology*, vol. 166, pp. 657–664, 1988.
[15] L. N. Bohs, S. C. Gebhart, M. E. Anderson, B. J. Geiman, and G. E. Trahey, "2-D motion estimation using two parallel receive beams," *IEEE Trans. Ultrason., Ferroelect., Freq. Contr.*, vol. 48, pp. 392–408, Mar. 2001.
[16] M. E. Anderson, "Multi-dimensional velocity estimation with ultrasound using spatial quadrature," *IEEE Trans. Ultrason., Ferroelect., Freq. Contr.*, vol. 45, pp. 852–861, May 1998.

Two Multichannel Integrated Circuits for Neural Recording and Signal Processing

Iyad Obeid*, James C. Morizio, Karen A. Moxon, Miguel A. L. Nicolelis, and Patrick D. Wolf

***Abstract*—We have developed, manufactured, and tested two analog CMOS integrated circuit "neurochips" for recording from arrays of densely packed neural electrodes. Device A is a 16-channel buffer consisting of parallel noninverting amplifiers with a gain of 2 V/V. Device B is a 16-channel two-stage analog signal processor with differential amplification and high-pass filtering. It features selectable gains of 250 and 500 V/V as well as reference channel selection. The resulting amplifiers on Device A had a mean gain of 1.99 V/V with an equivalent input noise of 10 μV_{rms}. Those on Device B had mean gains of 53.4 and 47.4 dB with a high-pass filter pole at 211 Hz and an equivalent input noise of 4.4 μV_{rms}. Both devices were tested *in vivo* with electrode arrays implanted in the somatosensory cortex.**

***Index Terms*—Integrated headstage, neural amplifier, neural recording, neurochip.**

I. Introduction

The rapidly expanding field of neuroprosthetics aims to interface artificial devices with the brain. Advancements in this field will require an increase in the number and density of simultaneously monitored electrodes implanted in multiple cortical and subcortical regions [1], [2]. A clear solution to this problem is to use custom designed analog integrated circuits (ICs) to acquire and process the electrical signals transduced from implanted extracellular cortical electrodes.

Manuscript received March 4, 2002; revised October 1, 2002. This work was supported by grants from Defense Advanced Research Projects Agency (DARPA), the Office of Naval Research (ONR), and the National Institutes of Health (NSF). *Asterisk indicates corresponding author.*

*I. Obeid is with the Department of Biomedical Engineering, Duke University, Durham, NC 27708 USA (e-mail: io@duke.edu).

J. C. Morizio is with the Department of Electrical and Computer Engineering, Duke University, Durham, NC 27708 USA.

K. A. Moxon is with the School of Biomedical Engineering, Science and Health Systems, Drexel University, Philadelphia, PA 19104 USA.

M. A. L. Nicolelis is with the Departments of Neurobiology and Biomedical Engineering, Duke University, Durham, NC 27708 USA.

P. D. Wolf is with the Department of Biomedical Engineering, Duke University, Durham, NC 27708 USA.

Digital Object Identifier 10.1109/TBME.2002.807643

Single-unit action potentials require signal processing to enhance the resolution of their arrival times and the differentiability of their waveform morphologies. Such signals must be buffered to reduce high source impedances and then amplified before being digitized. Bandpass filtering attenuates out-of-band biological and electrical noise, while high-pass filtering may attenuate low-frequency baseline drifts [3]. Published neural signal bandwidths range from 100–400 Hz to 3 k–10 kHz [2], [4], [5].

To explore the development of a single-chip hardware platform for neural data acquisition, two ICs were designed, fabricated, and tested. Device A was designed as a prototype headstage to investigate simple buffering and gain strategies, while Device B was used to investigate the integration of more advanced analog signal processing strategies customized for single units.

II. Methods

A. Device A

Device A is a 16-channel analog CMOS IC that amplifies and buffers signals taken directly from implanted neural electrodes. Each channel features a follower with a gain of 2 V/V formed from an opamp with two 20-kΩ feedback resistors [6]. Electrodes interface directly to the noninverting opamp inputs on each channel. Since these inputs are CMOS gates with picoamp leakage currents, the electrodes are not loaded. The voltage gain improves the signal-to-noise ratio (SNR) by reducing the relevance of electrical noise incurred in later stages. The gain of 2 V/V was selected for its potential for accurate implementation in silicon (to reduce gain variability across channels) and to limit the risk of saturation due to low-frequency electrode offsets. The opamp is a two stage amplifier with a P-type input differential pair operating from $\pm$2.5-V supplies. P-type devices were used for the differential pair (instead of N-type) for superior noise performance.

B. Device B

Device B is a 16-channel high-pass filter with a variable passband gain of either 250 or 500 V/V. The block diagram is shown in Fig. 1. The IC is divided into two sets of eight channels. Each channel consists of a variable gain high-pass filter cascaded into a single differential amplifier. The eight output signals from the variable gain filters of each eight-channel set are also wired to a 9 : 1 multiplexer. The ninth input on each of the multiplexers is the ground reference voltage, typically tied to a screw in the subject's skull [7]. The outputs of the two multiplexers are wired to the reference inputs of the eight differential amplifiers of the corresponding set of channels. The multiplexer allows the user to select between unipolar (ground reference) and bipolar (signal reference) recordings.

The architecture of the variable gain high-pass filters is seen in Fig. 2. Switch S may be closed to short R_{2b} and decrease the gain, while capacitor C gives the amplifier a high-pass filter characteristic with a dc gain of unity. The circuit was designed for a gain of 25 V/V or 50 V/V, with a high-pass filter pole at 217 Hz; the gain setting for all channels is determined by a single digital signal. Due to the prohibitive size of capacitors in silicon ($950 \cdot 10^{-18}$ F/μm^2 for our process) all 16 capacitors are placed off-chip. Designs using this circuit topology with smaller, integratable capacitors were rejected for noise concerns, as they would require resistors as large as tens of gigaohms to realize comparable gain and filter cutoffs. Our filter architecture combines a high input impedance with both gain and high-pass filtering, and requires only one additional input-output (I/O) per channel. The second section of Device B is a basic single-opamp differential amplifier with